$SmFe_{1-y}Co_yO_3$ Perovskite-Type Oxides For Soot Oxidation

Paritosh C Kulkarni, Satya Deepika Neelapala, Hari Prasad Uppara, Harshini Dasari, Nico Van Esch

ABSTRACT--- In the current study, a series of cobalt doped SmFeO3 perovskites (SmFe1-yCoyO3, y=0.1 to 0.35) were synthesized via EDTA-citrate method and used for soot removal applications. All the fabricated catalysts were characterized using XRD, SEM, BET surface area analysis and XPS analysis. It was found that the doping of Co into SmFeO3 perovskites considerable influences on morphology and soot oxidation reactions. The phase of the samples was investigated using XRD technique and examined the formation of orthorhombic phase till 30 mole% of Co-doped samples. All the samples exhibited low BET surface areas which are in the range of 2-6 m2/gm. From SEM analysis, the samples showed surface morphological changes with spherical shaped crystals. Sm existed in +3 oxidation states; Fe as +3 and Co as +3 in all the samples as evidenced from XPS results. Soot oxidation activity tests, investigated using TGA instrument and showed that SmFe0.7Co0.3O3-δ exhibited better catalytic performance (T50%- 496oC) when compared to un-doped SmFeO3 (T50% - 560oC).

Keywords— Perovskites, SmFe1-yCoyO3, Doping, Soot Oxidation, Adsorbed oxygen species.

1. INTRODUCTION

The diesel engine is an effective internal combustion engine extensively applied for motor vehicles and power generation because of its high power output and constant torque [1]. However, incomplete combustion of fuel leads to the emissions of particulate matter (PM) constituted mainly carbon, NOx, and hydrocarbons [2, 3]. The presence of these pollutants in the atmosphere leads to drastic climatic conditions, in turn, affect the human's life style. Therefore soot particulates are one of the most pressing harmful pollutants in the atmosphere [4].

To regulate these emissions, the new Euro VI standards propose to lessen the soot particles number to less than 6*1011 particles per kilometer [5]. Generally, the soot can be mitigated thermally at above 6000C involving high energy costs and complexity in operation [6, 7]. Thus many researchers find to develop novel technologies to abate the soot emissions, one among the most promising alternative technique is catalytic soot oxidation. Here, the soot can be oxidized in a diesel particulate filter fitted with a catalyst to meet the future targets.

Revised Manuscript Received on June 10, 2019.

Paritosh C Kulkarni, Department of Chemical Engineering, Manipal Academy of Higher Education, MIT, Manipal, Karnataka, 576104, India

Satya Deepika Neelapala, Department of Chemical Engineering, Manipal Academy of Higher Education, MIT, Manipal, Karnataka, 576104, India

Hari Prasad Uppara, Department of Chemical Engineering, Manipal Academy of Higher Education, MIT, Manipal, Karnataka, 576104, India

Harshini Dasari, Department of Chemical Engineering, Manipal Academy of Higher Education, MIT, Manipal, Karnataka, 576104, India. Tel.: +91 9177304954 (harshini.dasari@manipal.edu)

Nico Van Esch, University of Antwerp - Belgium

Perovskites have general formula ABX3 where A is alkali, alkaline, and rare-earth metals and B are transition metals [8]. The ionic size of 'A' elements is bigger than 'B' elements [9]. Perovskites have attracted numerous applications especially in the field of catalysis, solid-oxide fuel cells, solar applications, etc. Nowadays, perovskites have witnessed much attention due to its unique flexible nature of adopting different chemical properties of the periodic elements. These compounds exhibit high thermal stability and good chemical resistance towards the targeted substances [10]. Perovskite systems are widely used in catalytic applications due to its oxidation and reduction properties [8]. A catalyst possesses good catalytic activity due to the presence of its multiple oxidation states which in turn promotes to create oxygen vacancies (release of active surface adsorbed oxygen species) [11]. The surface adsorbed oxygen species are vitally required to carry out the oxidation reactions at lower temperatures. Many researchers attempting to explore new catalysts to operate it at better conditions.

Zhao et al [12] studied the effect of cobalt doping in SmFeO3 perovskite for the application on gas sensing. They concluded that large response and good selectivity to ethanol was showed by the sample when Co dopant level (y) reached 0.3. Torregrosa et al [13] synthesized copper doped BaMnO3 perovskite and concluded that BaMn0.7Cu0.3O3 exhibited active catalyst for soot oxidation. They also reported that the superior activity was due to the enhancement of the intrinsic reduction and oxidation properties of the catalyst due to the partial substitution of Mn+3/+4 by Cu+2 in the structure. Bukhari and co-workers [14, 15] prepared a series of Sm0.95Ce0.05Fe1-xCoxO3–δ perovskites and observed that as the Co content increases there is an increase in electrical conductivity of the samples, this is due to increase in the creation of more oxygen vacancies.

In the present study Co-substituted perovskite catalysts SmFe1-yCoyO3 (y=0.1 to 0.35) were prepared using EDTA-Citrate complex method. The synthesized catalysts were analyzed using different characterization techniques such as X-ray Diffraction technique (XRD), BET surface area, Scanning Electron Microscopy (SEM) and X-ray Photoelectron Spectroscopy (XPS). The investigation of the effect of Co substitution in the perovskite SmFeO3, on the catalytic soot oxidation activity, was studied using TGA instrument.

2. EXPERIMENTATION

2.1. Synthesis of catalysts:

Cobalt-doped perovskite $SmFe_{1-y}Co_yO_3$ (x = 0.1 to 0.35) was synthesized using EDTA/Citrate gel-based method. EDTA-citrate method [16, 17] has been chosen because of its simplicity, availability of the chemicals and it yields high purity of the materials. The materials used for the preparation of perovskites were of analytical grade such as $Sm(NO_3)_3{\cdot}6H_2O$ (99.9%, Alfa Aesar), $Fe(NO_3)_3{\cdot}9H_2O$ (≥98%, Molychem), $Co(NO_3)_2{\cdot}6H_2O$ (99.9%, Sigma-Aldrich), ethylene diamine tetra acetic acid (EDTA) (99%, Alfa Aesar), citric acid monohydrate (≥99%, Merck). Stoichiometric amounts of nitrates of the redox (Fe, Co) and non-redox metals(Sm) are mixed together to form a uniform solution. The metal nitrates, EDTA and citric acid are taken in the stoichiometric ratio of 1:1:1.5. EDTA is first dissolved in a concentrated NH_4OH for better solubility before it is added to the solution as well. Solid anhydrous citric acid was added to the resultant aqueous mixture and further NH_4OH solution was added to maintain pH as 10 for the complexation reaction to occur. The solution is then heated at 250 °C and stirred at 200 rpm until it forms a gel. This gel is then placed in an oven at 150°C for 3-4 hours where the mixtures will combust. The solid precursor was calcined at 800^0 C/10 h in a muffle furnace to obtain the final perovskite phase powder product. All the samples thus obtained were labeled as SFCy, where y is the mole% of Co doping (y=0, 10, 20, 30 and 35) in all the figures.

2.2. Characterization techniques

XRD technique can be used to analyze the structural phases of the samples. The phase analysis was carried out using Rigaku Miniflux 6000 instrument with high-intensity monochromatic Cu - Kα radiation of wavelength 1.54 A° at the rate of 0.003°/sec in the diffraction angle range of 10° to 60°. The crystallite size of the as-synthesized samples was evaluated using Debye Scherrer equation.

$$L = \frac{0.89\lambda}{\beta \cos\theta}$$

Where L is crystal size in nm, β is full width half maximum, λ is the wavelength of monochromatic x-ray and θ is diffraction angle.

The topology and surface morphology of the synthesized compounds were carried out in Hitachi S-1460 instrument.

The BET surface area of the as-prepared materials was determined using the instrument SmartSorb surface area analyzer. Initially, the samples are dried at 200 °C and also the sample was allowed to flow inert N_2 gas to remove any residual moisture.

XPS characterization technique was carried out in Thermo scientific K-Alpha instrument with Mg-Kα X-ray monochromator with the radiation of 1253.6 eV was used to obtain the high-resolution chemical state of the elements. This technique helps to examine the surface valence states of the elements present in the perovskites.

2.3. Catalytic Soot Oxidation Activity

The catalyzed soot oxidation reactions were evaluated using TA 55 thermogravimetric analyzer. Typically, 20 mg of the sample was loaded in the instrument and recorded the weight loss with respect to time and temperature. Initially, the sample was flushed in inert N_2 atmosphere up to 200°C to get rid of the excess moisture present on the surface of catalyzed soot. Then the sample is exposed to the zero grade air at a gas flow rate of 60 mL/min in the temperature range of 200 – 700 ^{0} C at a ramp input rate of 10^0 C/min. The model soot used for this analysis is Printex - U, obtained from Degussa. Here, the soot and catalyst in the mass ratio of 1:4 are mixed under tight contact using electric mortar and pestle for 15 min. The performance of catalysts was evaluated in terms of $T_{50\%}$, the temperature at which 50% conversion of the soot was achieved.

3. RESULTS AND DISCUSSIONS

3.1. XRD technique

Figure 1 depicts the diffraction patterns of the synthesized samples. Single phase $SmFeO_3$ with no phase segregation and any other stoichiometry like $Sm_3Fe_5O_{12}$ is successfully obtained at a calcination temperature of 900°C. Bragg Reflections of un-doped $SmFeO_3$ and Co-doped samples found to be in perfect correlation with the standard powder diffraction data (JCPDS: 39-1490) and assigned as orthorhombic structure. From the XRD patterns of $SmFe_{1-y}Co_yO_{3-\delta}$ (y=0.1, 0.2, 0.3 and 0.35), it can be concluded that the phase is changed gradually upon increasing the amount of dopant (Co). The absence of respective oxides Sm_2O_3, FeO_x, CoO_x, or any other impurities confirms the formation of $SmFe_{1-y}Co_yO_{3-\delta}$ solid solutions. Furthermore, the peaks are moved to a higher angle 2θ angle as shown in Fig.1 when compared to the peaks of pure $SmFeO_3$. This could be due to the lattice contraction of $SmFeO_3$ crystal because of the incorporation of lower ionic radii ions Co^{+3} (0.078nm), than the host ions Sm^{+3} (0.096nm) [14]. It can be noted that the major diffraction peak at ≈ 32° was divided when the dopant level (*y*) concentration reached to 0.35. It could be due to variation in pore size or lattice voids where dopant was being placed.

The calculated values of crystal size, crystal volume and lattice parameters of the as-prepared samples are displayed in **Table 1**. As the Co dopant level increased there is a decrease in the average crystal size and also cell volume due to the shrinkage of $SmFeO_3$ lattice. $SmFe_{0.7}Co_{0.3}O_{3-\delta}$ sample is found to have the lowest crystal size and cell volume.

Table 1: Crystal size, cell volume and surface area of $SmFe_{1-y}Co_yO_{3-\delta}$ samples

y	FWHM (°)	2θ (°)	Crystal Size (L) nm	V (nm^3)	Surface Area (m^2/g)
0.00	0.2279	32.33	35.89	0.2360	6.57
0.10	0.2460	32.50	33.26	0.2335	2.72
0.20	0.6500	32.58	12.59	0.2331	3.3
0.30	0.7897	32.98	10.37	0.2326	6.33
0.35	0.5522	32.98	14.84	0.2338	4.43

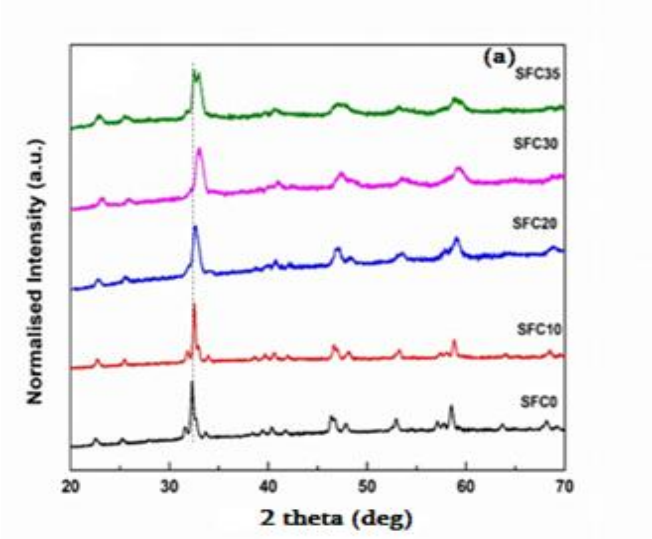

Fig.1. XRD Patterns of (a) (20-70°) range (b) (30-40°) 2θ range of the samples

3.2. SEM analysis

The morphology of the Co-doped $SmFeO_3$ perovskite materials was studied by Scanning Electron Microscopy (SEM). All these perovskite oxides shown in **Fig.2** exhibited aggregates with uniform aggregates with pores existing on the surface which is a general morphology of oxides.

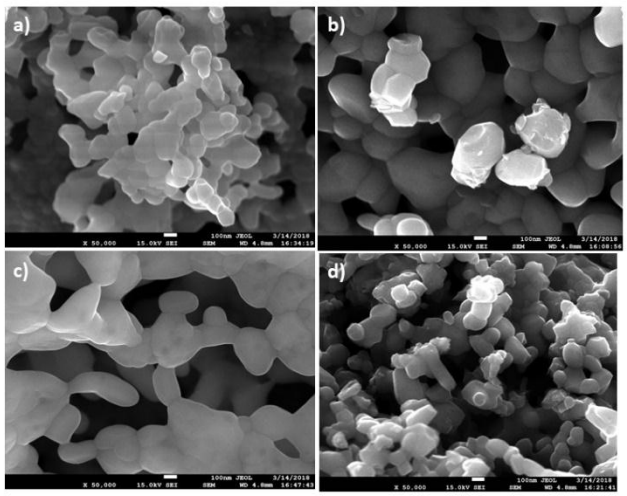

Fig. 2. SEM micrographs of the samples a) $SmFe_{0.9}Co_{0.1}O_{3-\delta}$ b) $SmFe_{0.8}Co_{0.2}O_{3-\delta}$ c) $SmFe_{0.7}Co_{0.3}O_{3-\delta}$ d) $SmFe_{0.65}Co_{0.35}O_{3-\delta}$

3.3. XPS Analysis

XPS technique is used for the measurement and identification of valence states with the help of peaks of Sm3d, Fe2p, Co2p, and O1s core levels as shown in Figure 3-6. According to the reported literature, the binding energy of Sm 3d is found to be around 1084 eV for Sm^{3+}. The Fig. 3 depicts peaks around 1082eV and 1112 for $Sm3d_{5/2}$ and $Sm3d_{3/2}$ multiplets respectively, corresponding to +3 oxidation state of Sm in all the samples [14, 15, 18]. The observed $Fe2p_{3/2}$ peak at 710 eV with spin-orbital splitting $Fe2p_{1/2}$ at 722.5 eV corresponds to the presence of +3 oxidation state of Fe in all the samples [14, 19, 20] as shown in Fig. 4. The chemical state of cobalt in the samples is determined through XPS of Co2p core level region. In Fig.5, Co $2p_{3/2}$ and Co $2p_{1/2}$ are further de-convoluted into two peaks, respectively. The Co $2p_{3/2}$ peak at 780 eV and the Co $2p_{1/2}$ peak at around 795 eV with the spin-orbit splitting difference of 15 eV can be attributed to the Co^{3+} oxidation state [12, 21, 22].

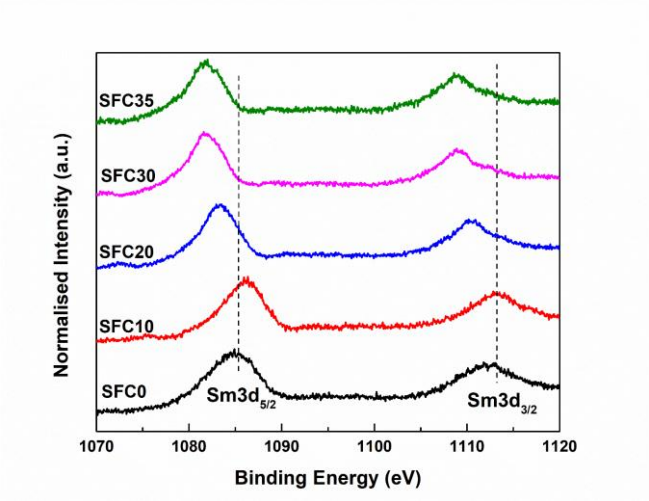

Figure. 3. XPS of Sm3d region of all the samples

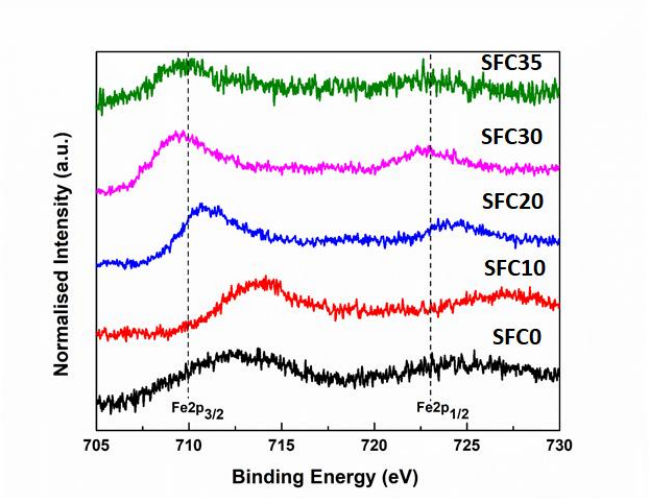

Fig. 4. XPS of Fe2p region of all the samples $SmFe_{1-y}Co_yO_{3-\delta}$ (y = 0.1, 0.2, 0.3 and 0.35).

Figure 6 represents the O1s peaks of the as-synthesized samples obtained through XPS analysis. The O1s peaks are characterized into two peaks and identified the peaks centered at around 529 eV and 531 eV respectively. The peak with binding energy from 529-530 eV can be attributed to lattice oxygen (α) and the peak from 530-532eV ascribed to adsorbed oxygen species (β) [23]. From the figure, O_α and O_β peaks of the sample $SmFe_{0.65}Co_{0.35}O_{3-\delta}$ appears at the lowest binding energy which signifies the bounded adsorbed oxygen species can be easily released. It implies that active mobile oxygen species responsible for soot oxidation are easily available in case of $SmFe_{0.65}Co_{0.35}O_{3-\delta}$ sample.

Published By:
Blue Eyes Intelligence Engineering
& Sciences Publication

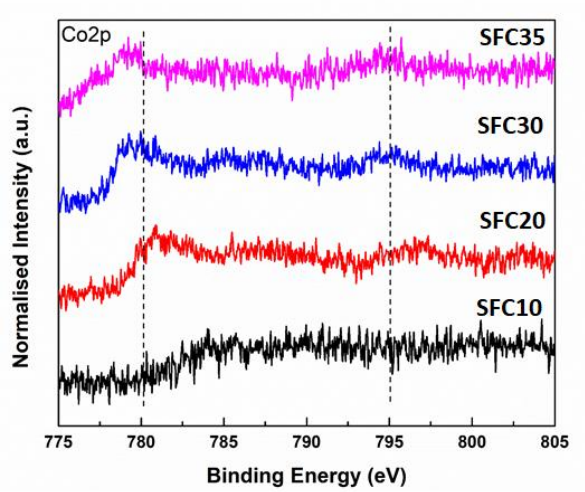

Fig. 5. XPS of Co2p region of all the samples $SmFe_{1-y}Co_yO_{3-\delta}$ (y = 0.1, 0.2, 0.3 and 0.35)

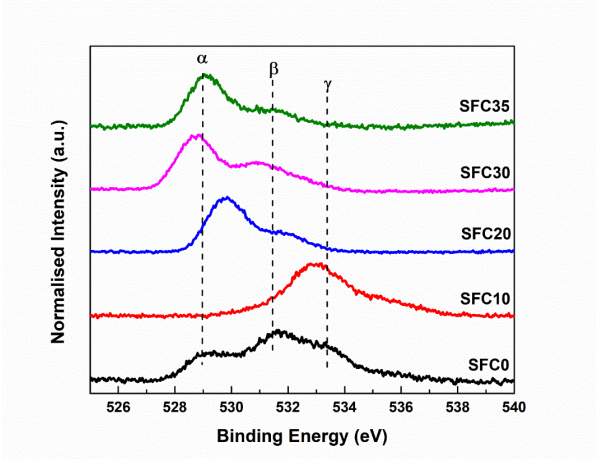

Fig.6. XPS of O1s region of all the samples $SmFe_{1-y}Co_yO_{3-\delta}$ (y=0, 0.1, 0.2, 0.3 and 0.35)

3.4. Soot Oxidation Activity

Figure 7 depicts the soot conversion v/s temperature of the un-catalyzed and catalyzed soot (with $SmFeO_3$ and Co-doped samples) under tight conditions. The temperature $T_{50\%}$ i.e, the temperature at which the 50% of the soot is oxidized is summarised in **Table 4.** $T_{50\%}$ values are in the order of $SmFe_{0.7}Co_{0.3}O_{3-\delta}$<$SmFe_{0.8}Co_{0.2}O_{3-\delta}$<$SmFe_{0.9}Co_{0.1}O_{3-\delta}$<$SmFe_{0.65}Co_{0.35}O_{3-\delta}$<$SmFeO_3$<Soot. The soot oxidation results indicate that the Co-doped samples exhibited the most favorable catalytic activity towards soot when compared with the un-doped $SmFeO_3$. Among all the doped samples, $SmFe_{0.7}Co_{0.3}O_{3-\delta}$ showed enhanced catalytic activity. This could be due to loosely bound oxygen species as evidenced by the XPS analysis (Fig. 6).

Table 2: The $T_{50\%}$ soot conversion temperatures of the samples

Compound	$T_{50\%}$
Soot	614
$SmFeO_3$	560
$SmFe_{0.9}Co_{0.1}O_{3-\delta}$	543
$SmFe_{0.8}Co_{0.2}O_{3-\delta}$	521
$SmFe_{0.7}Co_{0.3}O_{3-\delta}$	496
$SmFe_{0.65}Co_{0.35}O_{3-\delta}$	545

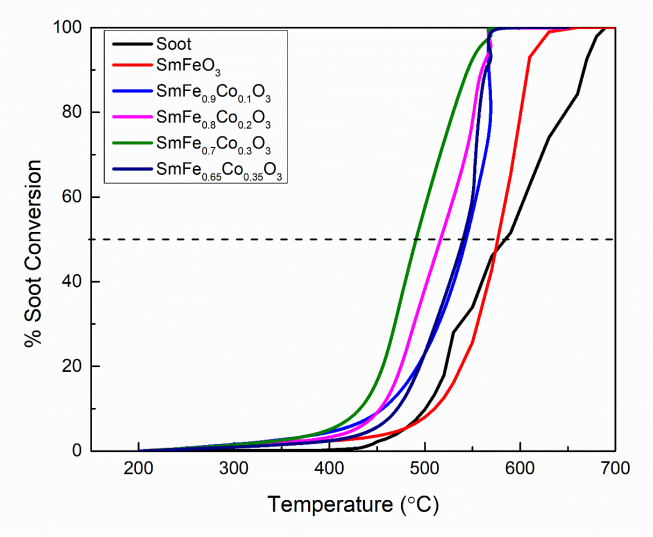

Fig. 7. Soot Conversion profiles of the samples $SmFe_{1-y}Co_yO_{3-\delta}$ (y= 0, 0.1, 0.2, 0.3 and 0.35)

4. CONCLUSIONS

The perovskite-type materials $SmFe_{1-y}Co_yO_{3-\delta}$ (y=0.1, 0.2, 0.3 and 0.35), synthesized using EDTA-citrate method tested these catalysts for soot oxidation reaction. All the prepared samples possessed a single-phase orthorhombic structure. The decrease of lattice parameters, crystal volume, and the crystal size was noticed with an increase in the Co content due to the creation of oxygen vacancies in the samples. SEM analysis revealed that all the samples exhibited similar morphology and specific surface area of the samples did not impose any effect on the soot oxidation activity. From XPS analysis Sm showed +3 oxidation state, Fe as +3 and Co as +3 in all the samples. Soot oxidation studies were performed using TGA instrument, showed that $SmFe_{0.7}Co_{0.3}O_{3-\delta}$ exhibited better catalytic performance ($T_{50\%}$ - 496^oC) when compared to un-doped $SmFeO_3$ ($T_{50\%}$ - 560^oC) because of the readily available active oxygen species.

REFERENCES

1. Mingjiao Tian, Chi He, Yanke Yu, Hua Pan, Louise Smith, Zeyu Jiang, Ningbo Gao, Yanfei Jian, Zhengping Hao, Qing Zhu. "Catalytic oxidation of 1,2-dichloroethane over threedimensional ordered meso-macroporous Co_3O_4 /$La_{0.7}Sr_{0.3}$Fe0.5Co0.5O3 : Destruction route and mechanism", Applied Catalysis A: General, 2018
2. Matti Maricq M (2007) Chemical characterization of particulate emissions from diesel engines: A review. J Aerosol Sci 38:1079–1118. https://doi.org/10.1016/j.jaerosci.2007.08.001
3. Adler J (2005) Ceramic diesel particulate filters. Int J Appl Ceram Technol 2:429–439. https://doi.org/10.1111/j.1744-7402.2005.02044.x
4. Niessner R (2014) The many faces of soot: Characterization of soot nanoparticles produced by engines. Angew Chemie - Int Ed 53:12366–12379. https://doi.org/10.1002/anie.201402812
5. Mendoza-Villafuerte P, Suarez-Bertoa R, Giechaskiel B, et al (2017) NOx, NH3, N2O and PN real driving emissions from a

Euro VI heavy-duty vehicle. Impact of regulatory on-road test conditions on emissions. Sci Total Environ 609:546–555. https://doi.org/10.1016/j.scitotenv.2017.07.168

6. Chi He, Jie Cheng, Xin Zhang, Mark Douthwaite, Samuel Pattisson, Zhengping Hao. "Recent Advances in the Catalytic Oxidation of Volatile Organic Compounds: A Review Based on Pollutant Sorts and Sources", Chemical Reviews, 2019
7. Di Sarli V, Landi G, Lisi L, et al (2016) Catalytic diesel particulate filters with highly dispersed ceria: Effect of the soot-catalyst contact on the regeneration performance. Appl Catal B Environ 197:116–124. https://doi.org/10.1016/j.apcatb.2016.01.073
8. Royer S, Duprez D, Can F, et al (2014) Perovskites as substitutes of noble metals for heterogeneous catalysis: Dream or reality. Chem Rev 114:10292–10368. https://doi.org/10.1021/cr500032a
9. Marchetti L, Forni L (1998) Catalytic combustion of methane over perovskites. 15:179–187
10. Liu S, Wu X, Weng D, Ran R (2015) Ceria-based catalysts for soot oxidation: A review. J Rare Earths. https://doi.org/10.1016/S1002-0721(14)60457-9
11. Huang X, Zhao G, Wang G, Irvine JTS (2018) Synthesis and applications of nanoporous perovskite metal oxides. Chem Sci 9:3623–3637. https://doi.org/10.1039/c7sc03920d
12. Zhao M, Peng H, Hu J, Han Z (2008) Effect of Cobalt doping on the microstructure, electrical and ethanol-sensing properties of SmFe1-xCoxO3. Sensors Actuators, B Chem 129:953–957. https://doi.org/10.1016/j.snb.2007.10.012
13. Satya Deepika Neelapala, Harsh Patnaik, Harshini Dasari. " Enhancement of soot oxidation activity of manganese oxide (Mn O) through doping by the formation of Mn M O (M = Co, Cu, and Ni) ", Asia-Pacific Journal of Chemical Engineering, 2018
14. Bukhari SM, Giorgi JB (2010) Effect of cobalt substitution on thermal stability and electrical conductivity of Sm0.95Ce0.05FeO3 - δin oxidizing and reducing conditions. Solid State Ionics 181:. https://doi.org/10.1016/j.ssi.2010.01.017
15. Bukhari SM, Giorgi JB (2011) Gases. 158:159–164
16. Anantharaman AP, Dasari HP, Dasari H, Babu GUB (2018) Surface morphology and phase stability effect of Ceria-Hafnia (CHx) binary metal oxides on soot oxidation activity. Appl Catal A Gen 566:181–189. https://doi.org/10.1016/j.apcata.2018.08.019
17. Shao Z (2000) Investigation of the permeation behavior and stability of a $Ba_{0.5}Sr_{0.5}Co_{0.8}Fe_{0.2}O_{3-\delta}$ oxygen membrane. J Memb Sci 172:177–188. https://doi.org/10.1016/S0376-7388(00)00337-9
18. Asamoto M, Harada N, Iwamoto Y, et al (2009) Catalytic activity of multi-metallic perovskite-type oxide prepared by the thermal decomposition of heteronuclear cyano complex, Sm[FexCo1-x(CN)6] . nH2O. Top Catal 52:823–827. https://doi.org/10.1007/s11244-009-9233-1
19. Bukhari SM, Giorgi JB (2009) Tuneability of Sm(1 - x)CexFeO3 ± λperovskites: Thermal stability and electrical conductivity. Solid State Ionics. https://doi.org/10.1016/j.ssi.2008.12.002
20. Levasseur B, Kaliaguine S (2009) Effects of iron and cerium in La1-yCeyCo1-xFexO3perovskites as catalysts for VOC oxidation. Appl Catal B Environ 88:305–314. https://doi.org/10.1016/j.apcatb.2008.11.007
21. Twagirashema I, Engelmann-Pirez M, Frere M, et al (2007) An in situ study of the NO + H2+ O2reaction on Pd/LaCoO3based catalysts. Catal Today 119:100–105. https://doi.org/10.1016/j.cattod.2006.08.013
22. Itagaki Y, Mori M, Hosoya Y, et al (2007) O3and NO2sensing properties of SmFe1-xCoxO3perovskite oxides. Sensors Actuators, B Chem 122:315–320. https://doi.org/10.1016/j.snb.2006.06.001

Published By:
Blue Eyes Intelligence Engineering
& Sciences Publication